International Journal of Thermal Sciences 49 (2010) 901–908

Contents lists available at ScienceDirect

International Journal of Thermal Sciences

journal homepage: www.elsevier.com/locate/ijts

On heat transfer in external natural convection flows using two nanofluids

C. Popa [a,*], S. Fohanno [a], C.T. Nguyen [b], G. Polidori [a]

[a] Laboratoire de Thermomécanique – GRESPI, EA 4301, Université de Reims Champagne – Ardenne, Moulin de la Housse, BP 1039, 51687 Reims, France
[b] Faculty of Engineering, Université de Moncton, Moncton, NB, Canada E1A 3E9

ARTICLE INFO

Article history:
Received 22 May 2009
Received in revised form
10 September 2009
Accepted 25 December 2009
Available online 1 February 2010

Keywords:
Natural convection
Water–alumina nanofluid
Water–CuO nanofluid
Heat transfer
Laminar–turbulent transition
Transition threshold

ABSTRACT

In the present work, a theoretical model based on the integral formalism approach for both laminar and turbulent external natural convection is extended to nanofluids. By using empirical models based on experimental data for computing viscosity and thermal conductivity of water–alumina and water–CuO suspensions, a close attention is first focused on the influence due to increasing the volume fraction of nanoparticles on the heat transfer and then to the transition threshold between laminar and turbulent regimes. The heat transfer is shown to strongly depend on the flow regime and on particle volume fraction. A clear degradation of heat transfer is observed using nanofluids while compared to that of the base-fluid. Moreover, the fact of increasing the particle volume fraction tends to delay the occurrence of the flow transition to turbulence.

1. Introduction

The application of additives to base liquids in the sole aim to increase the heat transfer coefficient is considered as an interesting mean for thermal systems. Nanofluids, prepared by dispersing nanometer-sized solid particles, have been extensively studied for more than a decade due to the observation of an interesting increase in thermal conductivity compared to that of the base-fluid [1,2]. Consequently, many researchers have focused their investigations on the way to increase the thermal conductivity by modifying the particle volume fraction, the particle size/shape or the base-fluid [3–5]. In a recent work [6], numerical results have eloquently shown that the use of Newtonian nanofluids for the purpose of heat transfer enhancement in natural convection was not obvious, as such enhancement is dependent not only on nanofluids effective thermal conductivities but on their viscosities as well. In fact, the effect of the kinematic viscosity has been found to be dominant in external natural convection heat transfer. In this same work, the authors have used two different viscosity models, namely one model proposed by Brinkman [7] currently used in literature for natural convection flows [8,9] and a more recent one proposed by Maïga et al. [10,11] to provide a better modelling of such nanofluids. The examination of the effect of these two models led to some contradictory conclusions. This means that an exact determination of the heat transfer parameters is not warranted as long as the question of the choice of an adequate and realistic effective viscosity model is not resolved. It is worth mentioning that this viewpoint is also confirmed in a recent work [12] for forced convection, in which the authors indicated that the assessment of the heat transfer enhancement potential of a nanofluid is difficult and closely dependent on the way the nanofluid properties are modelled.

Another feature concerning the use of nanofluids in convective flows is that, unlike forced convection, there is a striking lack of theoretical and experimental data in natural convection. The aim of the present study is to enhance the discussion on the use of nanofluids and also to add more information on natural convection heat transfer. First, this paper concerns the study of heat transfer when adding nanoparticles. Secondly, this paper deals with the laminar–turbulent transition in natural convective flows, and focuses on the effects of nanofluids on the transition threshold. Such effects, to our knowledge, have not yet been studied.

The present theoretical analysis is restricted to nanofluids and based on a macroscopic modelling under the assumption of constant thermophysical properties. The nanofluids considered for this study, at ambient temperature, are water–γAl_2O_3 and water–CuO suspensions composed of solid alumina nanoparticles with diameter of 47 nm ($\rho_p = 3880$ kg/m^3) and solid copper oxide nanoparticles with diameter of 29 nm ($\rho_p = 6500$ kg/m^3) with water as base-fluid. Results are presented only for particle volume fractions up to 10%, as no experimental data could be found in the literature concerning the rheological behavior of this nanofluid for higher particle volume fractions.

* Corresponding author. Tel.: +33 326913278; fax: +33 326913250.
E-mail address: catalin.popa@univ-reims.fr (C. Popa).

1290-0729/$ – see front matter © 2010 Elsevier Masson SAS. All rights reserved.
doi:10.1016/j.ijthermalsci.2009.12.015

Nomenclature

a	thermal diffusivity $m^2\ s^{-1}$
Cp	specific heat capacity $J\ kg^{-1}\ K^{-1}$
d	diameter m
g	acceleration of the gravity $m\ s^{-2}$
h	heat transfer coefficient $W\ m^{-2}\ K^{-1}$
k	thermal conductivity $W\ m^{-1}\ K^{-1}$
k_B	Boltzman constant $J\ K^{-1}$
l	mean free-path m
Nu	Nusselt number
Pr	Prandtl number $(=\mu C_p/k)$
Ra^*	modified Rayleigh number
Re	Reynolds number
T	temperature K
U	x velocity $m\ s^{-1}$
V	y velocity $m\ s^{-1}$
V_{Br}	Brownian velocity of nanoparticles $m\ s^{-1}$
x, y	parallel and normal to the vertical plane m

Greek symbols

β	coefficient of thermal expansion K^{-1}
δ	dynamical boundary layer thickness m
δ_T	thermal boundary layer thickness m
Δ	thermal to velocity layer thickness ratio
ϕ	particle volume fraction %
φ	heat flux density $W\ m^{-2}$
μ	dynamic viscosity Pa s
ν	kinematic viscosity $m^2\ s^{-1}$
ρ	density $kg.m^{-3}$
Θ	temperature °C

Subscripts

c	critical state
bf	base-fluid
f	fluid
nf	nanofluid
p	nanoparticle
r	ratio nanofluid/base-fluid
w	wall

2. Mathematical modelling

2.1. Assumptions and justification

The physical system considers a steady free convection boundary layer along a vertical wall heated with a uniform heat flux density. Both laminar and turbulent regimes, as well as the resulting transition threshold have been analyzed in the present approach. The theoretical model, based on the integral formalism, assumes sufficiently small temperature gradients across the boundary layer, so that thermophysical properties of the nanofluids are assumed to be constant except for the density variation in the buoyancy force, which is based on the incompressible fluid Boussinesq approximation. Since the solid particles have reduced dimension (<50 nm) and are believed to be easily fluidized, these particles can be considered to have a fluid-like behavior [1,10]. One may expect that the classical theory for single-phase fluids can be extended to nanofluids.

Because knowledge of nanofluids are still at their early stages, it seems very difficult to have a precise idea on the way the use of nanoparticles acts in natural convection heat transfer and complementary works are needed.

2.2. Estimation of nanofluid properties

The thermophysical properties of the nanofluids, namely the density, volume expansion coefficient and heat capacity have been computed using classical relations developed for a two-phase mixture [1,13,14]:

$$\rho_{nf} = (1-\phi)\rho_{bf} + \phi\rho_p \tag{1}$$

$$\beta_{nf} = (1-\phi)\beta_{bf} + \phi\beta_p \tag{2}$$

$$(\rho C_p)_{nf} = (1-\phi)(\rho C_p)_{bf} + \phi(\rho C_p)_p \tag{3}$$

It is worth noting that for a given nanofluid, simultaneous measurements of conductivity and viscosity are missing. In the present study, the dynamic viscosity is obtained from the relationship proposed by Maïga et al. [10,11] for water–γAl_2O_3 nanofluid (Eq. (4)) and Nguyen et al. [15] for water–CuO nanofluid (Eq. (5)), and derived from experimental data:

$$\mu_{nf} = \mu_{bf}(123\phi^2 + 7.3\phi + 1) \tag{4}$$

$$\mu_{nf} = \mu_{bf}(0.009\phi^3 + 0.051\phi^2 - 0.319\phi + 1.475) \tag{5}$$

With regard to the effective thermal conductivity of nanofluids, numerous experimental data as well as several theoretical models can be found in the literature. The development of accurate theoretical models taking into account all influencing parameters is still an active research area. Several possible mechanisms, such as Brownian motion or particle clustering [16] to name a few, have been proposed to explain the observed strong increase in the thermal conductivity. As an example of the diversity of the models proposed in the literature, two models are presented below and compared with experimental data for a water–alumina nanofluid.

The first model, proposed by Maxwell [17], assumes spherical particles homogeneously dispersed in the base-fluid. The nanofluid effective thermal conductivity is then given by:

$$k_{nf} = k_{bf}\frac{k_p + 2k_{bf} - 2\phi(k_{bf} - k_p)}{k_p + 2k_{bf} + \phi(k_{bf} - k_p)} \tag{6}$$

The second model [18] is a semi-empirical model aiming at taking into account possible effects of the Brownian motion on the resulting effective thermal conductivity. This is done through the following correlation:

$$k_{nf} = k_{bf}\left[1 + 64.7\phi^{0.746}\left(\frac{d_{bf}}{d_p}\right)^{0.369}\left(\frac{k_p}{k_{bf}}\right)^{0.7476}\mathrm{Pr}_{bf}^{0.9955}\mathrm{Re}^{1.2321}\right] \tag{7}$$

where the Reynolds number is based on the Brownian velocity (V_{Br}) of the nanoparticles, which is defined in [18]:

$$\mathrm{Re} = \frac{\rho_{bf}V_{Br}d_p}{\mu_{bf}} = \frac{\rho_{bf}k_BT}{3\pi l_{bf}(\mu_{bf})^2} \tag{8}$$

where l is the mean free-path and k_B is the Boltzman constant.

Most recently, Mintsa et al. [19] proposed the following correlation based on experimental data for the water−γAl_2O_3 nanofluid (Eq. (9)) and for the water−CuO nanofluid (Eq. (10)):

$$k_{nf} = k_{bf}(1.72\phi + 1.0) \tag{9}$$

$$k_{nf} = k_{bf}(1.74\phi + 0.99) \tag{10}$$

The effective thermal conductivities given by these three models for alumina−water nanofluids (Eqs (6), (7) and (9)) are plotted in Fig. 1 as functions of the nanoparticle volume fraction. One may observe that Chon et al. model [18] shows a good agreement with experimental data except a slight discrepancy for low particle volume fractions, whereas Maxwell's model strongly overestimates the thermal conductivity of the nanofluid. Moreover, we find that for two nanofluids (i.e. water−γAl_2O_3 nanofluid and water−CuO nanofluid), there is an increase of the thermal conductivity ratio of 15% for a particle volume fraction of 10%. Indeed, no definitive model is yet available as there are still debates on the mechanisms responsible for the modification of the conductivity [20]. Therefore the present study will only use the experimental model of Mintsa et al. [19] for the nanofluid thermal conductivity.

2.3. Laminar modelling

The complete theoretical development associated with the integral formalism has been previously presented in details in [21,22] for the free convection laminar regime and in [23,24] for the turbulent regime analysis.

In the laminar case, the integral formalism is developed for $Pr > 0.6$ and based on the assumption that the thermal to dynamical layer thickness ratio ($\Delta = \delta_T/\delta$) is dependent only on the Prandtl number [21,22]. The resulting relation is found to be (see also [6]):

$$\Delta_{nf}^7 - \frac{799}{126}\Delta_{nf}^6 + \frac{225}{14}\Delta_{nf}^5 - \frac{134}{7}\Delta_{nf}^4 + \frac{20}{3}\Delta_{nf}^3 + \frac{10}{9Pr_{nf}} = 0 \tag{11}$$

Because the thermal situation is that of a uniform heat flux density problem, the local modified Rayleigh number (Ra^*) is used and defined as follows:

$$Ra^* = \frac{g\beta\varphi_W x^4}{k\nu^2}Pr \tag{12}$$

With this definition, the modified Rayleigh number based on the nanofluid properties (Ra^*_{nf}) is given by:

$$Ra^*_{nf} = \frac{g\beta_{nf}\varphi_W x^4}{k_{nf}\nu_{nf}^2}Pr_{nf} \tag{13}$$

or expressed using the base-fluid Rayleigh number (Ra^*_{bf}) as:

$$Ra^*_{nf} = Ra^*_{bf}\frac{\beta_r Pr_r}{k_r\nu_r^2} \tag{14}$$

where $\beta_r, k_r, \nu_r, Pr_r$ are the nanofluid/base-fluid ratio for the corresponding properties.

In such a way, calculations lead to the following expression of the local Nusselt number in the laminar domain:

$$Nu_{nf}|_{LAM} = \left[Ra^*_{bf}\frac{2}{27Pr_{nf}\Delta_{nf}^4(9\Delta_{nf}-5)}\frac{\beta_r Pr_r}{k_r\nu_r^2}\right]^{\frac{1}{5}} \tag{15}$$

2.4. Turbulent modelling

Assuming that the turbulent boundary layer starts from the leading edge of the wall, the time-averaged boundary layer equations for the conservation of mass, momentum and energy are given under the Boussinesq approximation [23] as:

$$\frac{\partial U}{\partial x} + \frac{\partial V}{\partial y} = 0 \tag{16}$$

$$U\frac{\partial U}{\partial x} + V\frac{\partial U}{\partial y} = g\beta\Theta + \frac{\partial}{\partial y}\left[(\nu + \nu_t)\frac{\partial U}{\partial y}\right] \tag{17}$$

$$U\frac{\partial \Theta}{\partial x} + V\frac{\partial \Theta}{\partial y} = \frac{\partial}{\partial y}\left[(a + a_t)\frac{\partial \Theta}{\partial y}\right] \tag{18}$$

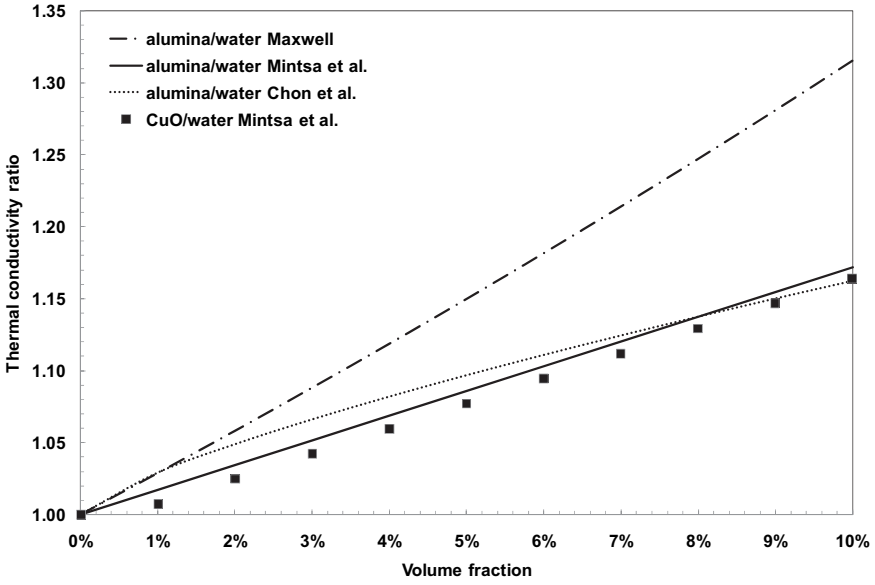

Fig. 1. Variation of the thermal conductivity ratio with the particle volume fraction.

where ν_t and a_t denote respectively the eddy diffusivity of both momentum and heat.

The present turbulent theory has been established under the assumption that the laminar boundary layer results could be extended to the turbulent regime so that relation (11) still remains valid [23,24].

The time-averaged integral forms of the boundary layer equations for the conservation of momentum and energy can be directly extended to nanofluids as (see again [23,24]):

$$\frac{\partial}{\partial x}\int_0^{\delta} U^2 \mathrm{d}y = g\beta \int_0^{\Delta\delta} \Theta \mathrm{d}y - (\nu + \nu_t)\left(\frac{\partial U}{\partial y}\right)_{y=0} \tag{19}$$

$$\frac{\partial}{\partial x}\int_0^{\Delta\delta} \Theta U \mathrm{d}y = -(a + a_t)\left(\frac{\partial \Theta}{\partial y}\right)_{y=0} \tag{20}$$

Where $\Delta = \delta_T/\delta$ still defines the thermal to dynamical boundary layer thickness ratio which is assumed to depend only on the Prandtl number.

Deriving the Colburn analogy and by using convenient wall shear stress under adequate velocity and temperature profiles [23,25] within the boundary layers give, after development and calculation, the turbulent Nusselt number as follows:

$$Nu_{\mathrm{nf}}|_{\mathrm{TURB}} = 0.0631\left(Ra^*_{\mathrm{bf}}\right)^{\frac{2}{7}}\left[\frac{\sqrt{\Pi_\Delta \mathrm{Pr}_{\mathrm{nf}}}}{\Delta_{\mathrm{nf}}}\left(1 + \frac{0.0823}{\Pi_\Delta \mathrm{Pr}_{\mathrm{nf}}^{\frac{10}{15}}}\right)\frac{k_r \nu_r^2}{\beta_r \mathrm{Pr}_r}\right]^{-\frac{2}{7}} \tag{21}$$

where Π_Δ is a function of Δ, the boundary layer ratio, given by:

$$\Pi_\Delta = \Delta_{\mathrm{nf}}^{\frac{8}{7}}\left(\frac{7}{72} - \frac{7}{60}\Delta_{\mathrm{nf}} + \frac{21}{253}\Delta_{\mathrm{nf}}^2 - \frac{14}{435}\Delta_{\mathrm{nf}}^3 + \frac{7}{1332}\Delta_{\mathrm{nf}}^4\right) \tag{22}$$

2.5. Transition threshold

Because of the lack of a physical criterion to define the transitional region, the present theoretical criterion used for transition to turbulence is similar to that chosen in [26], in which the laminar–turbulent transition corresponds to the location where laminar and fully developed turbulent flows interact together. Furthermore, since the transition is not a mathematical event, the most this analysis can do is to predict the order of magnitude of this transition.

Thus, the critical Rayleigh number can be obtained at the mathematical transition point by equalizing equations (15) and (21) and reporting the result into the expression (14). The critical Rayleigh number has been found dependent only on the nanofluid Prandtl number. Indeed, it is recalled that the boundary layer parameters Δ_{nf} and Π_Δ are also only Prandtl number dependent. The expression for the critical Rayleigh number is given by:

$$Ra^*_{\mathrm{nf}}|_c = 2.30 \times 10^{11}\left(\frac{k_r \nu_r^2}{\beta_r \mathrm{Pr}_r}\right)\left[\frac{\Pi_\Delta^5}{\mathrm{Pr}_{\mathrm{nf}}^2 \Delta_{\mathrm{nf}}^{38}(9\Delta_{\mathrm{nf}} - 5)^7} \times \left(1 + \frac{0.0823}{\Pi_\Delta \mathrm{Pr}_{\mathrm{nf}}^{\frac{10}{15}}}\right)^{10}\right]^{\frac{1}{3}} \tag{23}$$

3. Results and discussion

Because the theoretical modelling is based on the boundary layer equations in which the boundary layer thickness ratio (Δ) is assumed to be only Prandtl number dependent, Fig. 2 shows the evolution of the Prandtl number ratio ($\mathrm{Pr}_r = \mathrm{Pr}_{\mathrm{nf}}/\mathrm{Pr}_{\mathrm{bf}}$) with the particle volume fraction. It may be observed that, for the particle loading range considered ($0\% \le \phi \le 10\%$), the Prandtl number of water–alumina nanofluid strongly increases as the particle volume fraction increases and is nearly doubled for a particle volume fraction of 10%. As the Prandtl number is defined as $\mathrm{Pr} = \mu C_p/k$ therefore, such an increase of the nanofluid Prandtl number is essentially due to the strong augmentation of the nanofluid dynamic viscosity. In fact, this viscosity is almost tripled for $\phi = 10\%$ and overcomes largely the effects of the decreasing specific heat and increasing thermal conductivity, which tend to reduce the nanofluid Prandtl number. The results are curve-fitted

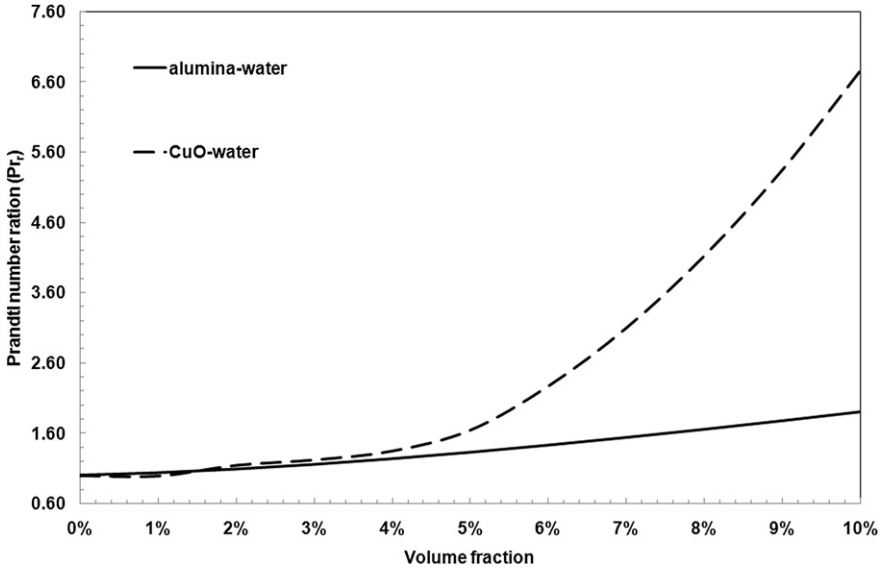

Fig. 2. Variation of the effective Prandtl number with the particle volume fraction.

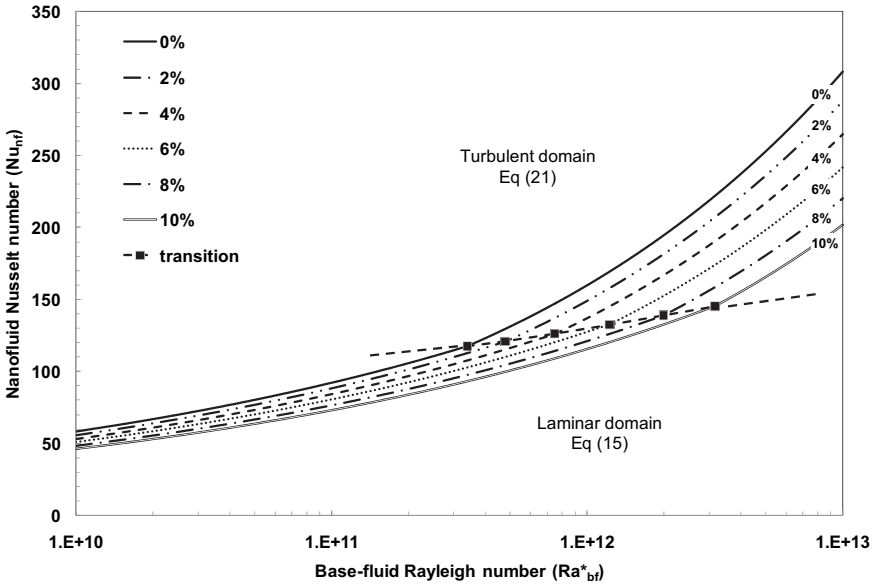

Fig. 3. Nusselt number for water−γAl_2O_3 nanofluid versus the base-fluid Rayleigh number.

with the following regression laws for water−γAl_2O_3 (Eq. (24)) and for water−CuO nanofluid (Eq. (25)):

$$\mathrm{Pr_r} = \frac{\mathrm{Pr_{nf}}}{\mathrm{Pr_{bf}}} = 50.2\phi^2 + 4.2\phi + 1 \tag{24}$$

$$\mathrm{Pr_r} = \frac{\mathrm{Pr_{nf}}}{\mathrm{Pr_{bf}}} = 904.5\phi^2 - 35.7\phi + 1.2 \tag{25}$$

Figs. 3 and 4 present the evolution of the local Nusselt number as a function of the base-fluid Rayleigh number (Ra^*_{bf}) and the particle volume fraction (ϕ). The evolutions are built by using Eq. (15) and Eq. (21) for the laminar and turbulent flow regimes, respectively. On the graph, a discontinuous line is used to represent the laminar-to-turbulent transition threshold; it is worth recalling that this threshold is based on a mathematical criterion corresponding to the intersection points of the two functions (15) and (21). It can be seen that when increasing the base-fluid Rayleigh number for a given particle fraction, the heat transfer parameter increases more steeply as the flow becomes turbulent, $\mathrm{Nu_{nf}} \sim (Ra^*_{bf})^{2/7}$ in the turbulent regime and $\mathrm{Nu_{nf}} \sim (Ra^*_{bf})^{1/5}$ in the laminar one.

It can also be observed that for a given Rayleigh number, the addition of nanoparticles result in a systematic decrease of the Nusselt number. For instance, for laminar regime with $Ra^*_{bf} = 10^{10}$ and a particle volume fraction of 10% a decrease of the Nusselt number by 21% and 37% are noticed for alumina–water and CuO–water nanofluids, respectively. For turbulent regime with $Ra^*_{bf} = 10^{13}$ and

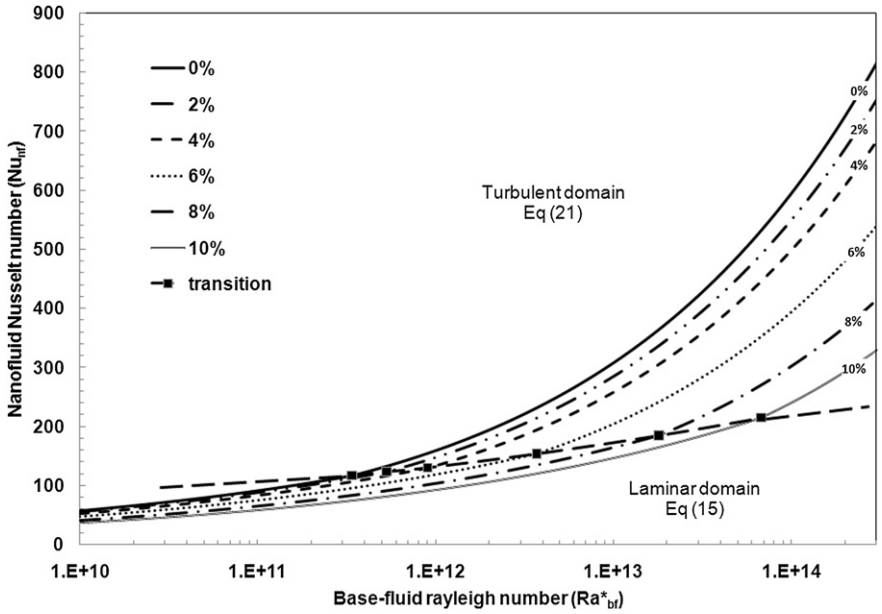

Fig. 4. Nusselt number for water−CuO nanofluid versus the base-fluid Rayleigh number.

Table 1
Variation of Ra^*_{nf} as a function of particle volume fraction for a base-fluid (water at 20 °C) at critical conditions ($Ra^*_{bf} = Ra^*_c$) and comparison with Ra^*_c.

ϕ(%)	Water−γAl_2O_3 nanofluid			Water−CuO nanofluid		
	Pr	Ra^*_{nf}	Ra^*_c	Pr	Ra^*_{nf}	Ra^*_c
0	6.98	3.40×10^{11}	3.40×10^{11}	6.98	3.40×10^{11}	3.40×10^{11}
1	7.22	3.58×10^{11}	3.95×10^{11}	6.95	3.38×10^{11}	3.48×10^{11}
2	7.59	3.86×10^{11}	4.78×10^{11}	8.02	4.20×10^{11}	5.32×10^{11}
3	8.06	4.23×10^{11}	5.93×10^{11}	8.55	4.62×10^{11}	6.64×10^{11}
4	8.62	4.68×10^{11}	7.47×10^{11}	9.43	5.35×10^{11}	9.03×10^{11}
5	9.27	5.22×10^{11}	9.55×10^{11}	11.50	7.19×10^{11}	1.57×10^{12}
6	9.98	5.83×10^{11}	1.22×10^{12}	15.88	1.15×10^{12}	3.71×10^{12}
7	10.74	6.49×10^{11}	1.56×10^{12}	21.65	1.81×10^{12}	8.42×10^{12}
8	11.56	7.24×10^{11}	1.99×10^{12}	28.81	2.74×10^{12}	1.80×10^{13}
9	12.41	8.04×10^{11}	2.52×10^{12}	37.33	3.99×10^{12}	3.60×10^{13}
10	13.30	8.90×10^{11}	3.17×10^{12}	47.17	5.61×10^{12}	6.78×10^{13}

the same particle concentration ($\phi = 10\%$), the Nusselt number decreases by 35% for alumina−water nanofluid and by 52% for CuO−water nanofluids.

The discontinuous line in Fig. 3 also indicates that the increase of the particle volume fraction delays the transition to turbulence. In order to explain this delay, Table 1 shows the variation of the nanofluid Prandtl (Pr_{nf}) and Rayleigh (Ra^*_{nf}) numbers as functions of the particle volume fraction. In this table, the base-fluid conditions ($\phi = 0\%$)are those of water at 20 °C, and the heat flux and the position along the vertical wall are such that critical conditions ($Ra^*_{bf} = Ra^*_c$) are reached. Then, these conditions are maintained; only the particle volume fraction is changed. In addition, Table 1 provides a comparison of Ra^*_{nf} with the transition (i.e. critical) Rayleigh number Ra^*_c corresponding to the ϕ-dependent nanofluid Prandtl number. One may observe that, under the conditions of the present study (water at 20 °C and fixed heat flux and position along the vertical wall), modifications of fluid properties due to an augmentation of the particle volume fraction result in an increase of the nanofluid Rayleigh and Prandtl numbers. However, the transition Rayleigh number (Ra^*_c) increases faster than the nanofluid Rayleigh number (Ra^*_{nf}). This means that, when the particle volume fraction is increased, the transition will be obtained with a higher heat flux or further downstream in the boundary layer.

The application of Newton's law, $q'' = h(T_w - T_f)$, shows that the temperature increase at the wall is inversely proportional to the heat transfer coefficient. Therefore, for constant heat flux situations, the heat transfer coefficient is a key parameter since it is an indicator of the wall temperature increase. Figs. 5 and 6 show the evolution of the heat transfer coefficient ratio for several particle volume fractions as a function of the base-fluid Rayleigh number. By comparing the heat transfer coefficient of the two nanofluids with that of the base-fluid, we observe that, for a given wall heat flux, a reduction of the natural convective heat transfer coefficient is systematically found, both in the laminar and turbulent regimes. For example in Fig. 5, the heat transfer coefficient with water−alumina nanofluid is reduced by 7% in the laminar regime, and by 23% in the turbulent one, for a particle volume fraction of 10%. In the same way, we notice that for the water−CuO nanofluid, the heat transfer coefficient decreases by 26% in the laminar regime and 53% in the turbulent regime. This result appears to be consistent with that from a previous published work [27] in which the authors mentioned that, unlike conduction or forced convection, a systematic and definite deterioration in natural convective heat transfer had been found while using nanofluids. Furthermore, for a given heat flux, increasing the particle volume fraction induces an augmentation of the critical Rayleigh number, which results in a delay of the occurrence of the turbulent regime leading to an extension of the laminar flow regime (Fig. 5).

The apparent paradoxical behavior observed when increasing the particle volume fraction can be explained as follows. Adding solid nanoparticles is expected to increase the thermal conductivity, thus resulting in higher heat transfer. However, an augmentation of the particle volume fraction also increases the mixture viscosity. For the natural convection flow of this study, it appears that the effect of increased viscosity is dominant over the increase of thermal conductivity. Therefore, it is expected that the buoyancy-induced flow transition to turbulence be delayed, which leads to a degradation of heat transfer. It is interesting to mention that this degradation of heat transfer was also found in mixed convection [28].

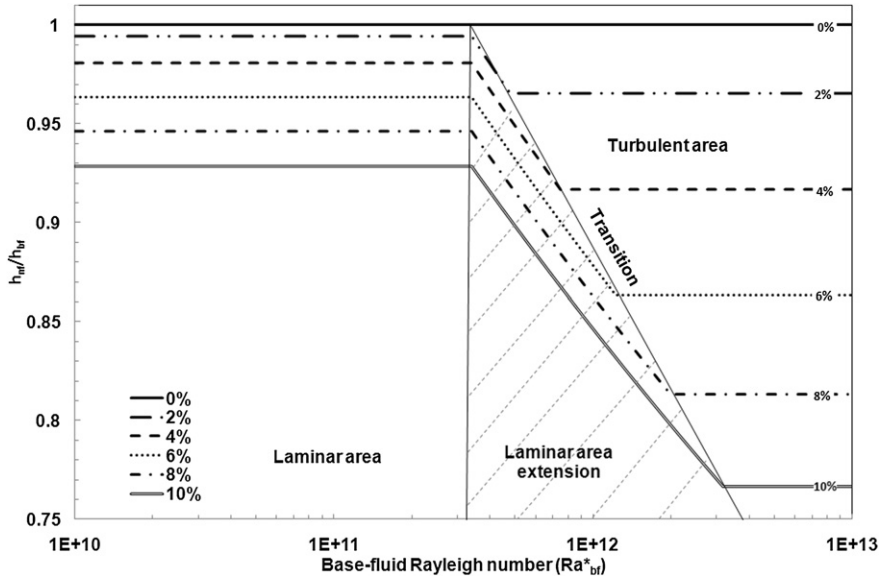

Fig. 5. Heat transfer coefficient ratio for water−γAl_2O_3 nanofluid versus the base-fluid Rayleigh number.

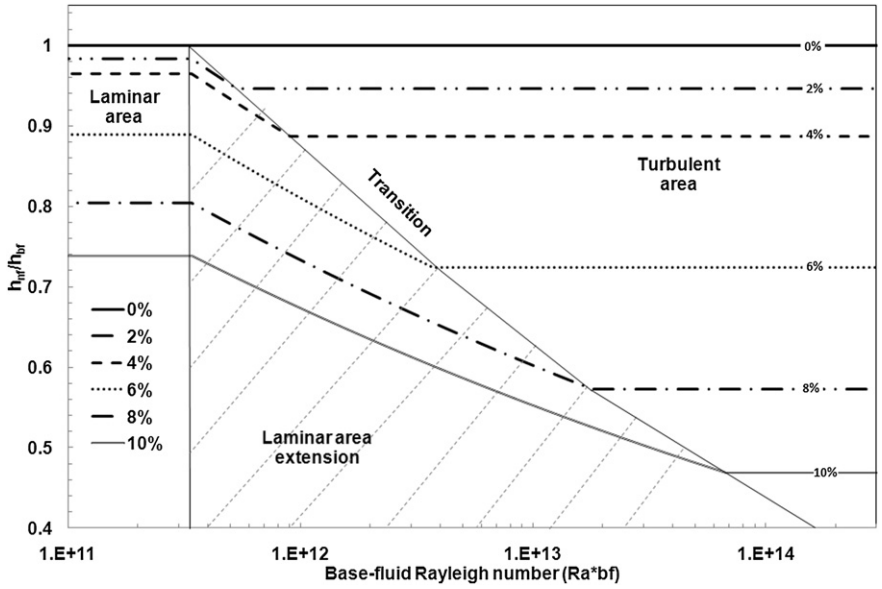

Fig. 6. Heat transfer coefficient ratio for water–CuO nanofluid versus the base-fluid Rayleigh number.

4. Conclusion

The laminar and turbulent natural convection boundary layer flow along a vertical wall subjected to a uniform heat flux condition has been theoretically investigated for water–γAl_2O_3 and water–CuO nanofluids and particle volume fractions up to 10%. The modelling is based on the integral formalism taking into account distinct thicknesses of the thermal and dynamical boundary layers, and by assuming that laminar results can be extended to the turbulent regime. The approach is based on the assumption of single-phase homogeneous fluid model and the use of experimental data for the dynamical viscosity and the thermal conductivity.

Increasing the nanoparticle volume fraction leads to a strong increase of the nanofluid Prandtl number for both nanofluids. This is essentially due to the strong increase of the dynamic viscosity. As concerns the heat transfer capacities of the nanofluids, they strongly depend on the flow regime and the particle volume fraction. A clear degradation of heat transfer is observed when using nanofluids while compared to that observed with the base-fluid. For the constant heat flux condition of the present study, it has been found that for a 10% volume fraction, the nanofluid heat transfer coefficient (h_{nf}) is almost reduced by 7% for water–γAl_2O_3 nanofluid and by 26% for water–CuO nanofluid in laminar regime and by 23% for water–γAl_2O_3 nanofluid and by 53% for water–CuO nanofluid in turbulent regime when compared to that of the base-fluid.

In addition to the degradation of heat transfer, it is also observed that adding nanoparticles in the base-fluid results in a systematic delay of the transition to turbulence. Finally, the results of the present study indicate that the use of nanofluids for heat transfer enhancement purposes does not seem feasible in a case of constant heat flux-induced external free convection flow.

References

[1] Y. Xuan, W. Roetzel, Conceptions for heat transfer correlation of nanofluids. Int. J. Heat Mass Transf. 43 (2000) 3701–3707.
[2] Y. Xuan, Q. Li, Heat transfer enhancement of nanofluids. Int. J. Heat Fluid Flow 21 (2000) 58–64.
[3] S.M.S. Murshed, K.C. Leong, C. Yang, Enhanced thermal conductivity of TiO_2–water based nanofluids. Int. J. Therm. Sci. 44 (2005) 367–373.
[4] M.S. Liu, M.C.C. Lin, I.-Te Huang, C.C. Wang, Enhancement of thermal conductivity with CuO for nanofluids. Chem. Eng. Technol. 29 (1) (2006) 72–77.
[5] Y.J. Hwang, Y.C. Ahn, H.S. Shin, C.G. Lee, G.T. Kim, H.S. Park, J.K. Lee, Investigation on characteristics of thermal conductivity enhancement of nanofluids. Curr. Appl. Phys. 6 (2006) 1068–1071.
[6] G. Polidori, S. Fohanno, C.T. Nguyen, A note on heat transfer modelling of Newtonian nanofluids in laminar free convection. Int. J. Therm. Sci. 46 (2007) 739–744.
[7] H.C. Brinkman, The viscosity of concentrated suspensions and solutions. J. Chem. Phys. 20 (1952) 571–581.
[8] L. Gosselin, A.K. da Silva, Combined heat transfer and power dispersion optimization of nanofluid flows. Appl. Phys. Lett. 85 (2004) 4160–4162.
[9] K. Khanafer, K. Vafai, M. Lightstone, Buoyancy-driven heat transfer enhancement in a two-dimensional enclosure using nanofluids. Int. J. Heat Mass Transf. 46 (2003) 3639–3653.
[10] S.E.B. Maïga, S.J. Palm, C.T. Nguyen, G. Roy, N. Galanis, Heat transfer enhancement by using nanofluids in forced convection flows. Int. J. Heat Fluid Flow 26 (2005) 530–546.
[11] S.E.B. Maïga, C.T. Nguyen, N. Galanis, G. Roy, T. Maré, M. Coqueux, Heat transfer enhancement in turbulent tube flow using Al_2O_3 nanoparticle suspension. Int. J. Numer. Methods Heat Fluid Flow 16 (3) (2006) 275–292.
[12] R. Ben Mansour, N. Galanis, C.T. Nguyen, Effect of uncertainties in physical properties on forced convection heat transfer with nanofluids. Appl. Therm. Eng. 27 (2007) 240–249.
[13] B.C. Pak, Y.I. Cho, Hydrodynamic and heat transfer study of dispersed fluids with submicron metallic oxide particles. Exp. Heat Transf. 11 (2) (1998) 151–170.
[14] S.-Q. Zhou, R. Ni, Measurement of specific heat capacity of water-based Al_2O_3 nanofluid. Appl. Phys. Lett. 92 (2008) 093123.
[15] C.T. Nguyen, F. Desgranges, G. Roy, N. Galanis, T. Maré, S. Boucher, H. Angue Mintsa, Temperature and particle-size dependent viscosity data for water-based nanofluids – *Hysteresis phenomenon*. Int. J. Heat Fluid Flow 28 (2007) 1492–1506.
[16] P. Keblinski, S.R. Philpot, S.U.S. Choi, J.A. Eastman, Mechanisms of heat flow in suspensions of nano-sized particles. Int. J. Heat Mass Transf. 45 (2002) 855–863.
[17] J.C. Maxwell, A Treatise on Electricity and Magnetism. Clarendon Press, Oxford, 1873.
[18] C.H. Chon, K.D. Kihm, S.P. Lee, S.U.S. Choi, Empirical correlation finding the role of temperature and particle size for nanofluid (Al_2O_3) thermal conductivity enhancement. Appl. Phys. Lett. 87 (2005) 153107.
[19] H.A. Mintsa, G. Roy, C.T. Nguyen, D. Doucet, New temperature dependent thermal conductivity data for water-based nanofluids. Int. J. Thermal Sci. 48 (2009) 363–371.
[20] D. Wen, G. Lin, S. Vafaei, K. Zhang, Review of nanofluids for heat transfer applications. Particuology 7 (2009) 141–150.
[21] G. Polidori, E.C. Mladin, T. de Lorenzo, Extension de la méthode de Karman-Pohlhausen aux régimes transitoires de convection libre pour Pr $>$ 0.6. C.R. Acad. Sci. Paris Sér. IIb (328) (2000) 763–766.
[22] G. Polidori, C. Popa, T.H. Mai, Transient flow rate behaviour in an external natural convection boundary layer. Mech. Res. Commun. 30 (2003) 615–621.

[23] C. Varga, S. Fohanno, G. Polidori, Turbulent boundary-layer buoyant flow modeling over a wide Prandtl number range. Acta Mechanica 172 (2004) 65–73.
[24] C. Popa, S. Fohanno, G. Polidori, Note on the turbulence transition threshold of a buoyancy-driven flow over an isothermal vertical wall. WSEAS Trans. Heat Mass Transf. 2 (2007) 1–5.
[25] S. Kakaç, Y. Yener, Convective Heat Transfer, second ed.. CRC Press, Boca Raton, 1995.
[26] V.S. Arpaci, S.H. Kao, Foundations of buoyancy driven heat transfer correlations. Trans. ASME J. Heat Transf. 123 (2001) 1181–1184.
[27] N. Putra, W. Roetzel, S.K. Das, Natural convection of nanofluids. Heat Mass Transf. 39 (2003) 775–784.
[28] R.B. Mansour, N. Galanis, C.T. Nguyen, Etude expérimentale de l'écoulement et du transfert de chaleur des nanofluides, in: Proc. CIFQ 2009, Lille, France, 18–20 may 2009, pp. 39–44.